

One Framework to Rule Them All: Unifying Multimodal Tasks with LLM Neural-Tuning

Hao Sun^a, Yu Song^b, Jiaqing Liu^b, Jihong Hu^b, Yen-Wei Chen^{b,*}, Lanfen Lin^{a,*}

^aCollege of Computer Science and Technology, Zhejiang University, Hangzhou, Zhejiang, China

^bCollege of Information Science and Engineering, Ritsumeikan University, Ibaraki, Osaka, Japan

Abstract

Large-scale models have exhibited remarkable capabilities across diverse domains, including automated medical services and intelligent customer support. However, as most large models are trained on single-modality corpora, enabling them to effectively process and understand multimodal signals remains a significant challenge. Current research often focuses on designing task-specific or scenario-specific tuning strategies, which limits the scalability and versatility. To address this limitation, we propose a unified framework that concurrently handles multiple tasks and modalities. In this framework, all modalities and tasks are represented as unified tokens and trained using a single, consistent approach. To enable efficient multitask processing, we introduce a novel tuning strategy termed neural tuning, inspired by the concept of sparse distributed representation in the human brain, where only specific subsets of neurons are activated for each task. Furthermore, to advance research in multimodal and multitask learning, we present a new benchmark, MMUD, which includes samples annotated with multiple task labels spanning reasoning segmentation, referring segmentation, image captioning, and text-to-image generation. By applying neural tuning to pretrained large models on the MMUD benchmark, we demonstrate the ability to handle multiple tasks simultaneously in a streamlined and efficient manner. All models, code, and datasets will be released publicly upon publication, fostering further research and innovation in this field.

Keywords: Multimodal learning, Large language models, Pretrained model tuning, Referring segmentation, Complex Segmentation, Image generation

1. Introduction

Recently, the rapid advancements in deep learning and hardware computing power have propelled the development of large-scale models, achieving significant breakthroughs in applications such as intelligent customer support and autonomous driving. The remarkable success of these models can be attributed to their large-scale architectures and extensive training data, which substantially enhance their contextual understanding and complex reasoning capabilities. However, most large-scale models are pretrained on single-modality corpora due to the challenges associated with acquiring large-scale multimodal datasets and the computational limitations of current hardware. To address this, recent research has explored enabling large language models (LLMs) to process multimodal data through fine-tuning. While these methods improve performance on specific tasks, they predominantly rely on task-specific architectures or tuning strategies (such as referring segmentation and image-text classification [1, 2, 3]), which significantly hinders their scalability and versatility in handling multiple tasks concurrently. Although expanding the capabilities of LLMs through more intricate architectures or tuning strategies is possible, this approach imposes considerable complexity and overhead, limiting the feasibility of extending such models to accommodate additional tasks or datasets.

In revisiting the human cognitive process, which serves as the inspiration for artificial intelligence, we observe that humans inherently excel at multitask learning and effortlessly adapt to new tasks. A key factor underpinning this ability is the principle of Sparse Distributed Representation (SDR), or the Sparse Coding Hypothesis (SCH),

*Corresponding Authors

which posits that information is represented in a way where only a small fraction of neurons are active at any given time [4, 5]. This principle is believed to enhance the efficiency of information processing and enable the brain to form unique and robust representations of complex data. Motivated by these findings in neuroscience, we propose a unified framework for multitask and multimodal learning in large language models (LLMs), as illustrated in Figure 1. Our framework introduces two key innovations:

Unified Tokenization for Multimodal Multitask Learning. We formulate all tasks, as well as their multimodal data inputs and outputs, into a unified token-based representation. Unlike previous approaches that rely on cross-attention mechanisms to facilitate multimodal interactions [6, 7], our framework directly feeds the tokenized inputs into the model, leveraging the pretrained model’s self-attention mechanism [8]. This allows the model to compute relationships across and within modalities in a holistic manner, enhancing its ability to understand inter- and intra-modal dependencies. By unifying tasks and modalities in this manner, we train all multimodal tasks simultaneously, enabling the model to capture shared patterns across different input data. This approach not only simplifies the tuning process but also mitigates task-specific biases, as the model learns to generalize from diverse input-output mappings. Consequently, our method allows pretrained models to handle multiple tasks with a single causal language modeling objective, significantly reducing computational overhead compared to prior methods.

Neural Tuning Strategy. To further improve the efficiency and adaptability of multimodal multitask learning, we introduce neural tuning, a novel tuning strategy inspired by SDR. In this strategy, only a subset of neurons is activated for each task, mimicking the sparse activation patterns observed in the human brain. Neurons activated by different tasks consist of two components: shared neurons, which capture common features across tasks, and task-specific neurons, which encode unique characteristics for individual tasks. This design not only enhances multitask learning efficiency but also reduces computational costs by selectively activating neurons. Furthermore, by avoiding additional cross-attention mechanisms and complex decoders, our framework ensures simplicity and computational efficiency while maintaining strong performance across tasks.

In summary, our framework seamlessly integrates multimodal and multitask learning into a unified architecture inspired by human cognitive principles, enabling efficient task handling with reduced computational requirements. Despite these advancements, there is currently a lack of datasets specifically designed for multimodal multitask learning, particularly for challenging tasks like reasoning segmentation, where multiple objects can only be segmented through complex reasoning that combines both image and textual information. To address this gap and foster progress in this domain, we introduce a novel dataset, MMUD (Multimodal Understanding Dataset). MMUD is constructed using GPT-4 to generate initial annotations, which are subsequently refined and verified through human annotation. The dataset comprises over 36,000 samples, each containing an image paired with a detailed content caption, a complex reasoning question-answer pair, and referring segmentation masks that align with object words in intricate descriptions. MMUD is explicitly designed to support diverse multimodal tasks that demand advanced reasoning and multimodal understanding. A comprehensive description of the dataset and its construction process is provided in Section 4. To demonstrate the capabilities of our framework, we fine-tune pretrained LLMs on MMUD for four distinct tasks: vanilla referring segmentation, reasoning segmentation, image captioning, and text-to-image generation. Figure 1 illustrates the pipeline of our proposed method, incorporating neural tuning. Experimental results indicate that our approach achieves state-of-the-art performance across these tasks, highlighting the effectiveness and generalizability of the framework.

Our contributions are threefold:

- We propose a novel framework that unifies diverse multimodal tasks using a concise all-in-token methodology. This approach simplifies the integration of new tasks by requiring only the introduction of task-specific tokens, significantly enhancing the flexibility and scalability of large multimodal models.
- We introduce neural tuning, a sparse task-tuning strategy inspired by Sparse Distributed Representation (SDR). This approach adaptively activates specific subsets of neurons for different tasks, enabling efficient multitask management while enhancing precision and adaptability across tasks.
- We present a new multimodal benchmark, MMUD, which includes meticulously annotated samples designed for multiple tasks, such as reasoning segmentation, image captioning, and text-to-image generation. By fine-tuning models on MMUD using our proposed framework, we demonstrate superior multitask and multimodal processing capabilities, setting a new state-of-the-art in performance.

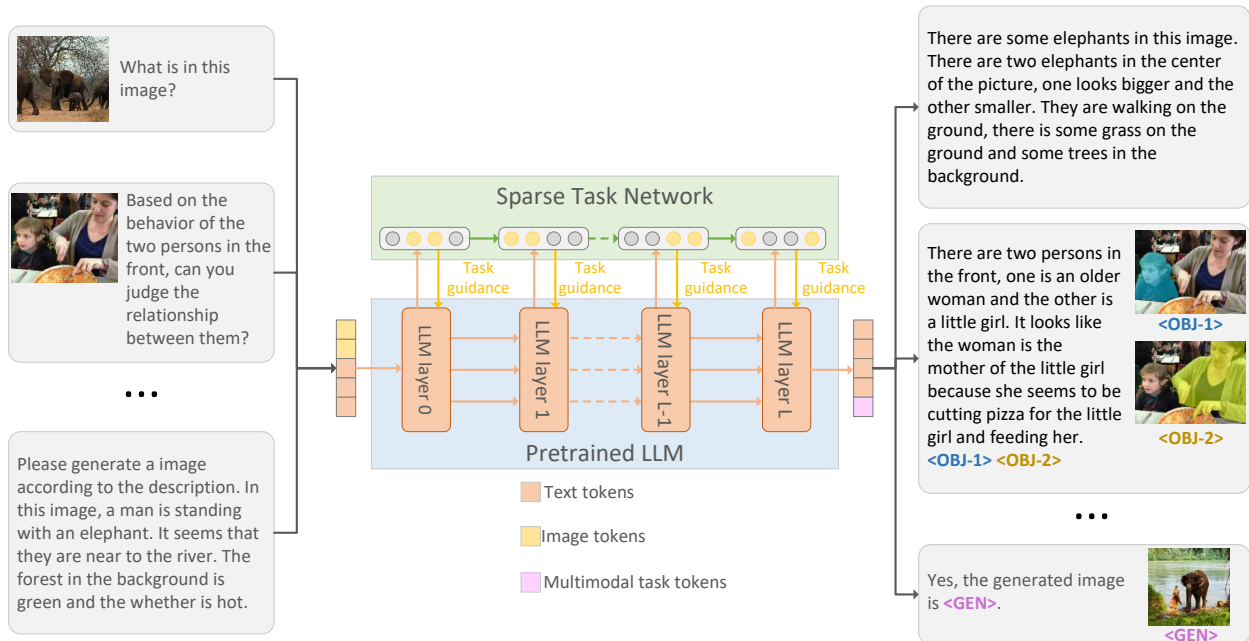


Figure 1: The overview of our proposed multitask and multimodal tuning framework. All inputs and outputs are token-based, encompassing both texts and images. The model generates specific tokens for different tasks, such as `<OBJ>` for segmentation and `<GEN>` for text-to-image generation. During tuning, a new sparse task network is introduced to emulate SDR and provide task guidance for pretrained LLMs. The entire LLM remains frozen, with only the newly introduced parameters being tunable.

The remainder of this paper is organized as follows. In Section 2, we review related works, focusing on advancements in multimodal learning, tuning strategies, and their applications in large language models. Section 3 presents our proposed unified framework, detailing its innovative all-in-token methodology and the neural tuning strategy for efficient multitask and multimodal learning. In Section 4, we introduce the MMUD dataset, describing its construction, annotation process, and utility for evaluating multitask and multimodal learning. Section 5 illustrates the experimental results and provides a comprehensive analysis of the proposed framework’s performance across various tasks. Finally, Section 6 concludes the paper by summarizing our contributions and discussing potential directions for future research.

2. Related Works

In this section, we analysis some recent or foundational works related to our method, including multimodal tuning, referring segmentation, and text-to-image synthesis.

2.1. Multimodal Tuning for Large Models

Recently, large models have demonstrated remarkable potential across diverse domains, not only in practical applications but also as tools for advancing scientific inquiry. However, training such models directly on multimodal data is often infeasible due to significant hardware and data constraints. To address this, various multimodal tuning strategies have emerged, primarily leveraging pre-trained language models to endow them with multimodal perception capabilities. The core concept of these approaches is to preserve the original model parameters by keeping them frozen, while adapting newly introduced components through lightweight methods such as adapters or specialized architectures. For example, Flamingo [9] retains a frozen image encoder and incorporates multimodal information via gated cross-attention, showcasing the ability of large language models (LLMs) to process multiple modalities. BLIP-2 [10], on the other hand, introduces the Q-Former module, a sophisticated mechanism designed to align image and text embeddings by extracting shared semantic representations, which has proven highly effective and widely

adopted. Similarly, FROMAGe [11] employs linear transformations to bridge textual and visual features, enabling seamless translation between these domains. More recently, vision-language LLMs (LVLMs) such as LLaVA [12] and Qwen-VL [13] have demonstrated exceptional multimodal reasoning and understanding capabilities. Our proposed framework and the novel neural tuning strategy build on the foundations of multimodal tuning for LLMs. However, our approach emphasizes multitask learning in a more elegant and concise manner, particularly excelling in reasoning and segmentation tasks under complex scenarios.

2.2. Referring Segmentation and Reasoning Segmentation

Among multimodal understanding tasks, referring segmentation is a foundational challenge that involves segmenting objects in an image based on textual instructions. This task evaluates a model’s ability to establish connections between fine-grained visual details and linguistic cues, making it a crucial benchmark for assessing multimodal understanding. Earlier approaches typically utilized a text encoder alongside a U-Net-like [14] vision backbone to produce segmentation masks, as exemplified by methods such as LAVT [15] and SLViT [6]. With the advent of large models, however, referring segmentation has become relatively trivial, as simple textual instructions fail to challenge the advanced reasoning capabilities of these models. To address this limitation, the concept of complex reasoning segmentation was introduced. This paradigm extends beyond basic segmentation by incorporating complex questions about image content that require sophisticated reasoning to answer. The output is not limited to segmentation masks but also includes detailed textual responses to these complex queries. Furthermore, the model must identify and segment the objects relevant to its answers. For example, LISA [16] introduced a novel architecture with specialized tokens for segmentation, while PixelLM [2] proposed a newly designed codebook to support multi-instance segmentation. In our work, reasoning segmentation is a pivotal task for evaluating the multimodal reasoning and processing capabilities of our framework.

2.3. Text-to-Image Synthesis

For text-to-image synthesis, there are generally two approaches highly related to our work: vector quantized generative adversarial network (VQGAN) related methods [17] and diffusion-based methods [3, 18]. VQGAN aims to map images into a discrete latent space while diffusion models simulates a diffusion process, where data is gradually transformed from a simple prior distribution (like Gaussian noise) to the complex target distribution. State-of-the-art text-to-image models such as GLIDE [19], DALL-E [20], and Imagen [21] leverage advanced techniques in VQGAN and diffusion models to generate high-quality, diverse images. In our work, we primarily employ VQGAN for synthesizing images, but we also explore the potential of combining our approach with diffusion networks for image generation.

3. Method

In this section, we first describe the detailed design of our framework with neural tuning, and then outline the specifics of multitask training.

3.1. All-in-token Multimodal Paradigm

The overall pipeline of our proposed neural tuning framework is illustrated in Figure 1. The inputs from the different modalities are tokenized and processed concurrently, emulating the ability of humans to seamlessly handle multiple tasks. We also introduce a novel sparse task network into pretrained models, which functions as either the Sparse Distributed Representation (SDR) or the Sparse Coding Hypothesis (SCH), through which only a subset of neurons are activated, tailored to the specific task at hand. This paradigm enables the model to take both image and text inputs, generating task-specific outputs such as multi-instance referring segmentation (<OBJ>) and image generation (<GEN>).

Specifically, for a multimodal input consisting of images and sentences, we first embed the text into $I_{txt} = \{I_{txt}^l\}_{l=1}^{L_t}$, where L_t denotes the length of the text. Next, we use a pretrained vision encoder to extract features from the image, resulting in $I_{img} = \{I_{img}^l\}_{l=1}^{L_i}$ where L_i representing the number of image patches. To integrate the multimodal input, we concatenate the text embeddings and image features (when the task requires visual input) to form the final input for the pretrained large language model (LLM): $I = [I_{img}; I_{txt}]$. In this scheme, the textual and visual modalities

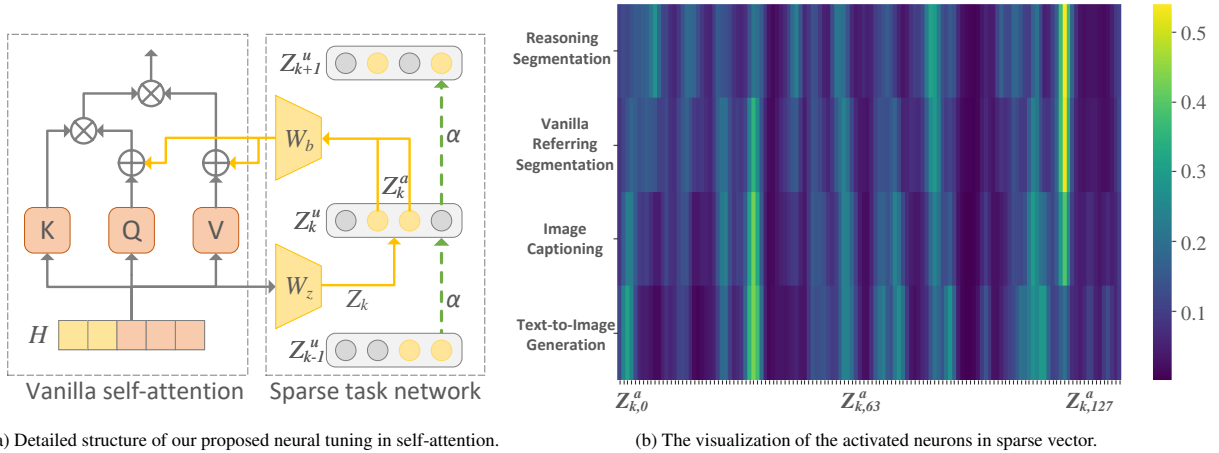


Figure 2: The detail of proposed neural tuning and the illustration of activated neurons in sparse vector. Figure (a) illustrates the integration of the sparse task network designed to generate task guidance for pretrained LLMs. At the core of the sparse task network is the sparse vector Z_k , with only a percentage of neurons activated to perform specific tasks. Sparse vectors across different layers are interconnected through an EMA updating mechanism. Figure (b) visualized the sparse vector Z_k^a for different tasks (D_z is set to 128 in the example).

interact through the LLM’s self-attention mechanism, where the output O is computed as $O = \text{SoftMax}(\frac{QK^T}{\sqrt{d_k}})V$ with the Query (Q), Key (K), and Value (V) derived from the concatenated multimodal input I . Unlike prior works that employ cross-attention for modality interaction [6, 15], where Q , K , and V are derived from different modalities, our self-attention approach offers several advantages. Not only does it simplify the architecture by avoiding explicit cross-modal mappings, but it also enables the model to compute both inter- and intra-modal relationships. This dual interaction within the self-attention framework enhances the model’s ability to understand and fuse multimodal information more effectively.

In the output stage of the LLM, we introduce new task-specific tokens alongside the original textual tokens to handle multimodal tasks. For example, we incorporate $\langle \text{OBJ} \rangle$ tokens for segmentation tasks and $\langle \text{GLB} \rangle$ tokens for text-to-image synthesis. These task-specific tokens are then fed into their respective decoders, enabling the model to generate the appropriate outputs for each task. This approach unifies the input and output format across all tasks into an all-in-token scheme, simplifying the integration of additional tasks and modalities. As a result, the system becomes more flexible and scalable, allowing for easy extension to new multimodal tasks without significant architectural changes.

3.2. Neural Tuning for Large Models

To fine-tune the pretrained LLMs, we introduce a sparse task network behaving like SDR. It is parallel to pretrained LLMs but gets linked in each layer for task guidance. For each tuning layer, it maintains a learnable vector named the *Sparse Vector* and the details are shown in Figure 2a. In the k -th layer of the LLM before self-attention, we first project the hidden embeddings H into a subspace to obtain the sparse vector:

$$Z_k = W_z H \in \mathbb{R}^{(L_r+L_i) \times D_z}, \quad (1)$$

where $H \in \mathbb{R}^{(L_r+L_i) \times D_h}$, $W_z \in \mathbb{R}^{D_z \times D_h}$ is a learnable matrix, D_h is the embedding size of the pretrained LLM, and D_z is the dimension of the sparse vector. To ensure the sparse vector is transmitted between layers, Z_k is updated using an Exponential Moving Average (EMA) mechanism with a hyperparameter α :

$$Z_k^u = \alpha Z_{k-1}^u + (1 - \alpha) Z_k, \quad (2)$$

where Z_{k-1}^u is the sparse vector from the last layer. This approach allows the sparse vector to not only receive information from the previous layer but also be aware of the current layer’s information. To enable sparse distributed representation during model flow, only a subset of the sparse vector’s nodes are activated for various tasks. We first

randomly sample an activation rate r from a normal distribution $p(r) = N(r; \beta, (0.1\beta)^2)$, where $\beta \in (0, 1)$ is a predefined hyperparameter¹. Then, we activate corresponding neurons as follows:

$$Z_{k,j}^a = \begin{cases} Z_{k,j}^u & Z_{k,j}^u \geq Z_{k,r}^u \\ 0 & Z_{k,j}^u < Z_{k,r}^u \end{cases} \quad (3)$$

where $Z_{k,r}^u$ is the largest top r values and $j \in [1, D_z]$. Z_k^a represents the activated neurons for a specific task. Next, to allow the pretrained LLM to leverage task-specific guidance, we use a linear transformation to project the activated sparse vector back to the LLM’s hidden space:

$$Z_k^b = W_b Z_k^a \in \mathbb{R}^{(L_l+L_i) \times (2D_h)}, \quad (4)$$

where W_b is a learnable parameter. For the self-attention mechanism of the LLM, we split Z_k^b into two parts and use the residual for query (Q) and value (V) computation,

$$\begin{aligned} Q' &= W_q H + Z_k^b[:, 0 : D_h], \\ V' &= W_v H + Z_k^b[:, D_h : 2D_h], \\ K &= W_k H. \end{aligned} \quad (5)$$

Q' , K , and V' are then employed for the vanilla self-attention in pretrained LLMs. Overall, the pretrained LLM is responsible for the main inference, while the sparse task network handles the execution of different tasks. Interestingly, our experiments reveal that more related tasks tend to activate a greater number of the same neurons (e.g., vanilla referring segmentation and reasoning segmentation). This finding highlights the relationship between different tasks, as illustrated in Figure 2b.

3.3. Multitask Training

As different tasks are unified into an all-in-one token manner, the tuning procedure can be conducted using a simple causal language modeling approach. Cross-entropy loss is employed as the loss function (\mathcal{L}_{txt}) for next-token prediction:

$$\mathcal{L}_{txt} = - \sum_t \log \hat{P}(x_t | x_i; i < t), \quad (6)$$

where $\hat{P}(x_t | x_i; i < t)$ is the predicted probability for the token x_t based on the context of all previous tokens.

For segmentation-related tasks, the embeddings corresponding to object tokens $\langle \text{OBJ} \rangle$, H_{seg} , are collected and fed to a lightweight decoder for corresponding mask generation:

$$\hat{y} = \text{Decoder}_{seg}(H_{seg}, W_{seg}), \quad (7)$$

where W_{seg} represents the learnable parameters in the mask decoder. Different from previous methods [16], which employ pretrained SAM [22] for predicting masks, our designed decoder is much lighter. The mask decoder consists of three convolutional layers for upscaling, each followed by three self-attention layers for mask decoding. Since the models can generate multiple segmentation tokens at a time, we can easily perform multi-instance segmentation. Following previous works [16, 2], DICE loss [23] is employed in our framework to guide the segmentation tasks:

$$\mathcal{L}_{seg} = \mathcal{L}_{DICE} = \frac{1}{N} \sum_i \left(1 - \frac{2|\hat{y}_i \cap y_{gt,i}|}{|\hat{y}_i| + |y_{gt,i}|} \right) \quad (8)$$

where N is the number of samples, \hat{y} is the predicted mask and y_{gt} is the ground truth.

In text-to-image synthesis tasks, we employ pretrained VQGAN generators [17, 24] to synthesize images. To generate a sequence of indices for VQGAN to produce images, we train a conditional transformer to predict the indices in an autoregressive manner:

$$p(\mathbf{s}|c) = \prod_i p(s_i | s_{<i}, c), \quad (9)$$

¹More activation patterns are discussed in Section 5.5

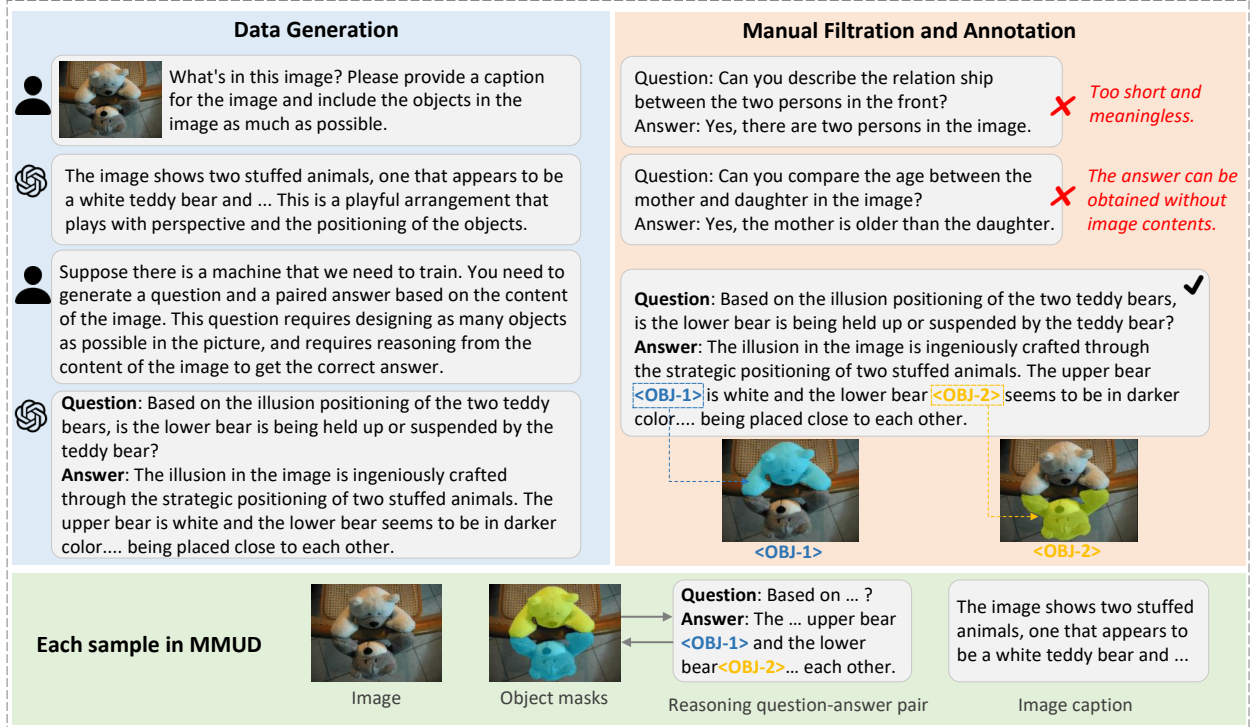


Figure 3: Pipeline for MMUD Dataset Generation. First, GPT-4v is used to generate captions describing the image contents and reasoning question-answer pairs. Then to ensure dataset quality, meaningless cases are filtered out. Finally, <OBJ> tokens are manually appended to objects in the answers to help large models better understand the relationships between images and text.

where s is the sequence of indices for VQGAN to generate images and c is the condition that controls the contents of the images. To simplify the tuning process, we first pretrain the conditional transformer on MS-COCO [25] and employ the image embeddings from the pretrained CLIP model [26] as the condition. After training, we can generate images via the CLIP embeddings. Therefore, in neural tuning, we simply align the embeddings of the synthesis tokens (H_{gen}) to the CLIP embeddings (H_{clip}). The mean squared error is employed to perform the alignment:

$$\mathcal{L}_{gen} = \mathcal{L}_{MSE} = \frac{1}{N} \sum_i (W_{gen} H_{gen} - H_{clip})^2, \quad (10)$$

where W_{gen} is a learnable transformation to project token embeddings into the CLIP feature space.

The pretrained LLMs are then tuned with all tasks involved. The overall training loss is represented as:

$$\mathcal{L} = \mathcal{L}_{txt} + \lambda_{seg} \mathcal{L}_{seg} + \lambda_{gen} \mathcal{L}_{gen}, \quad (11)$$

where λ_{seg} and λ_{gen} are coefficients to balance the numerical scales of different losses.

4. MMUD Benchmark

To enable LLMs with multitask and multimodal processing capabilities, a high-quality dataset is essential. However, there are few datasets that provide multitask annotations specifically designed for large models. To address this, we have constructed the MMUD dataset. MMUD dataset contains over 36,000 samples. We have divided the dataset into training, validation, and test subsets, comprising 33,682, 1,400, and 1,400 samples, respectively. Each sample in the dataset is annotated with referring segmentation masks, complex reasoning question-answer pairs, and image captions. In this work, we focus on four tasks with MMUD: vanilla referring segmentation, reasoning segmentation, image captioning and text-to-image generation.

We constructed our dataset using open-source datasets: RefCOCO [27], RefCOCOg [28], and RefClef [29, 28]. Since these datasets only provide referring segmentation masks, we augmented them with annotations for other tasks. The dataset generation pipeline is illustrated in Figure 3. Initially, we employed GPT-4v to generate image captions describing the contents. Subsequently, GPT-4v was used to generate complex questions along with answers based on the image contents. We then performed manual filtration to ensure that the generated contents were meaningful and suitable for multimodal understanding. We filtered out samples in cases where: 1) the generated contents were meaningless; 2) the length of the generated contents was either too long or too short; 3) the answers could be directly inferred from the questions without reference to the images. To enhance the capability of complex reasoning, we manually inserted the `<OBJ-i>` token after each object in the answer, where i represents the i -th object in the image. For example, when generating the question *Can you judge the relationship between the two people in the front based on what happened in the picture?* with the answer with answer *In this image, one of the women in the front is cutting a pizza, and a little girl is next to her...*, we manually inserted the `<OBJ>` token after the expression of each object: *In this image, one of the women in the front <OBJ-1> is cutting a pizza <OBJ-2>, and a little girl <OBJ-3> is next to her...* Following the structure of the RefCOCO datasets, each sample image contains multiple meaningful objects with corresponding masks. Each `<OBJ-i>` token not only corresponds to an object but also to the corresponding segmentation mask, which could help models better capture the relationship between texts and images. The dataset will be made publicly available to advance research in this area.

5. Experiments and Analysis

5.1. Experimental Settings

In our method, we employ the pretrained LLaMA2-13B and LLaMA2-7B as the textual foundation models. For image feature extraction, we utilize CLIP-ViT-L/14. The images are resized to 224 pixels as inputs. All parameters in LLaMA and CLIP are kept frozen, and only the newly introduced tokens, sparse task network, and task decoders are trainable (2.9% in total). The efficient parameter α in sparse vector updating is set to 0.9, while the neuron activation rate β is set to 0.4. We set the dimension of the sparse vector Z to 128. During optimization, to balance the numerical scales in the loss functions, we set λ_{seg} to 1.0 and λ_{gen} to 10.0. We train the models for 10 epochs with a batch size of 12 and a cosine learning rate decay scheduler. The tuning process takes about 36 hours on four RTX 4090 GPUs or three NVIDIA A100 GPUs.

5.2. Results on MMUD

Table 1 and Table 2 presents the results of our proposed neural tuning compared with previous methods. For vanilla referring segmentation and reasoning segmentation, we mainly compare our method with LVAT, LISA, and PixelLM. We employ the mean intersection over union (mIoU) and overall IoU as the metrics. LVAT aims to fuse the BERT features into vision backbones, achieving great results in vanilla segmentation. However, when it comes to complex reasoning scenarios, LVAT fails to converge while other LLM-based methods yield good results, demonstrating the powerful reasoning capabilities of large models. Compared with LISA and PixelLM, which employ pretrained LLaVA [12] and focus on complex reasoning segmentation, neural tuning can achieve better results, demonstrating its effectiveness. Regarding inference speed, our tuned 7B model can complete the reasoning segmentation process within 80ms per text-image pair on an RTX 4090 GPU, while the 13B model takes 110ms on an RTX A6000 GPU. This demonstrates the efficiency of our proposed neural tuning. We believe this efficiency results from the linear sparse vector updating and task guidance.

Furthermore, to further evaluate the effectiveness of our proposed method, we also present the performance on the original test set of RefCOCO, RefCOCO+, and RefCOCOg datasets ². As shown in Table 1b, our method achieves state-of-the-art performance on the public datasets but with lower computational burden, revealing the effectiveness and efficiency of our proposed multitask neural tuning for segmentation tasks.

For image captioning, we compare our method with BLIP-2 [10], ExpansionNetV2 [30] and mPLUG [31]. BLIP-2 proposed a Q-Former for multimodal interaction while mPLUG learn the relationship between modalities by cross-modality skip-connection. We employ the BLEU-4 [32], CIDEr [33], and METEOR [34] metrics for evaluation. The

²For fair comparison, we re-split the train, validation, and test set of MMUD according to the original datasets.

Table 1: The results our neural tuning (NT in table) and previous methods on MMUD and three public datasets for reasoning segmentation and referring segmentation.

(a) The results of reasoning segmentation on MMUD dataset. As MMUD is a new dataset, we re-implement the methods based on their open-source codes.

Method	w/ LLM	Valid		Test	
		mIoU	oIoU	mIoU	oIoU
LVAT		21.2	20.2	23.3	23.1
LISA-7B	✓	60.1	59.9	61.3	61.8
PixelLM-7B	✓	61.1	60.7	63.2	62.6
NT-7B(Ours)	✓	62.2	61.6	63.1	62.8
LISA-13B	✓	62.0	61.2	63.1	62.7
PixelLM-13B	✓	63.4	62.8	64.4	64.0
NT-13B(Ours)	✓	63.4	63.0	64.9	64.2

(b) The results of vanilla referring segmentation on RefCOCO, RefCOCO+, and RefCOCOg are presented. The metric used in the table is oIoU.

Method	w/ LLM	TFLOPs	RefCOCO			RefCOCO+			RefCOCOg(U)	
			Val	TestA	TestB	Valid	TestA	TestB	Valid	Test
LVAT			72.7	75.8	68.8	62.1	68.4	55.1	61.2	62.1
LISA-7B	✓	7.16	74.0	76.3	70.4	62.5	66.3	56.0	67.0	69.1
PixelLM-7B	✓	3.57	73.0	76.5	68.2	66.3	71.7	58.3	69.3	70.5
NT-7B(Ours)	✓	2.47	74.2	76.7	68.0	66.3	71.2	58.1	70.3	70.2

Table 2: The results our neural tuning and previous methods on MMUD for image captioning task and text-to-image generation task.

Image Captioning				Text-to-image Synthesis			
Method	BLEU-4	METEOR	CIDEr	Method	FID(↓)	KID(↓)	IS
BLIP2-6.7B	41.9	34.7	133.0	GLIGEN	12.9	12.5	31.1
ExpansionNetV2	41.1	34.0	132.7	U-ViT-S/2	13.7	15.9	29.8
mPLUG	43.0	34.1	134.0	Parti	11.0	13.6	30.6
NT-7B(Ours)	43.7	35.5	133.2	NT-7B(Ours)	12.7	15.2	31.4

results are shown in Table 2. As we can draw from the results, we can reach the competitive performance compared with previous state-of-the-art approaches.

On text-to-image synthesis tasks, quantitative metrics are shown in Table 2. We employ FID score [35], KID Score [36], and inception score (IS [37]) as the metrics. We compare our method with previous methods, including Parti [38], GLIGEN [39], and U-ViT-S/2 [40]. Compared with other methods, one of the significant advantage of our method is that neural tuning is designed for multitask tuning instead of a certain task.

5.3. Case Visualization

The visualizations of several cases generated by our model are shown in Figure 4. These cases encompass a variety of tasks, including vanilla referring segmentation, reasoning segmentation, image captioning, and image generation. For image generation, we utilize two pretrained decoders: VQGAN and DALL-E2. In the case of reasoning segmentation, the model not only accurately segments the corresponding objects but also provides detailed reasoning or explanations for the results. These examples highlight the model’s ability to seamlessly handle diverse multimodal tasks, demonstrating both its precision in segmentation and its creative capabilities in image generation.

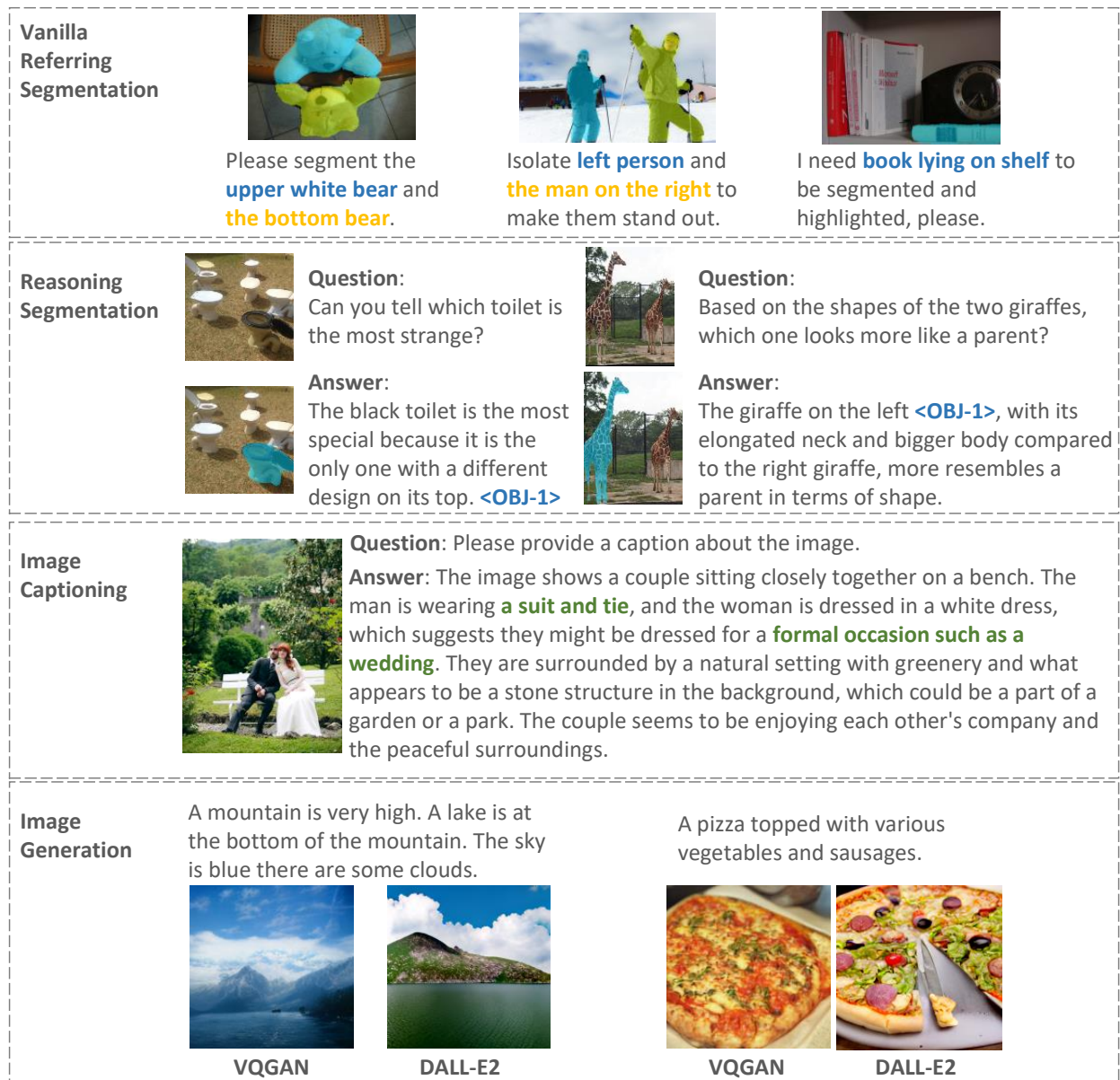


Figure 4: The visualization of some cases from our model, including vanilla referring segmentation, reasoning segmentation, image captioning, and image generation.

Table 3: The ablation study on MMUD test set for reasoning segmentation. The LLaMA2-7B is employed in the ablation. Z_k^U Upd. means the sparse vector updating module (Equation 2) and SDR indicates the sparse distributed representation emulation. Task V.S., Task I.C. and Task I.S. means the vanilla referring segmentation, image captioning and text-to-image synthesis tasks, respectively.

Z_k^U Upd.	Ablations			Tuning Modules			MMUD		
	SDR	Task V.S.	Task I.C.	Task I.S.	Q	K	V	mIoU	oIoU
✓					✓		✓	57.7	57.6
	✓				✓		✓	59.3	58.2
✓	✓				✓		✓	60.0	58.9
✓	✓	✓			✓		✓	61.1	50.7
✓	✓		✓		✓		✓	62.0	61.2
✓	✓			✓	✓		✓	62.9	62.6
✓	✓	✓	✓	✓	✓		✓	63.1	62.8
✓	✓	✓	✓	✓		✓	✓	62.0	61.1
✓	✓	✓	✓	✓	✓	✓	✓	63.5	63.0

5.4. Effectiveness of Self-Attention in All-in-token Paradigm

In our approach, we utilize self-attention to compute the attention scores between the various elements of the input, including both image patches and textual tokens. This differs from traditional methods that rely on cross-attention, where separate attention mechanisms are used for different modalities. The self-attention mechanism, by contrast, enables a more unified interaction between modalities, allowing the model to capture both intra-modal and inter-modal relationships simultaneously.

As shown in Figure 5, we visualize the attention scores between image patches and corresponding textual tokens for reasoning segmentation with relatively shorter sentences. The figure demonstrates that object-related words in the text (such as "cat," "car," or "tree") receive significantly higher attention weights from their corresponding image patches. This indicates that the self-attention mechanism effectively focuses on the relevant visual regions when processing the corresponding linguistic cues, facilitating a more coherent integration of multimodal information. The ability to compute these attention scores in a unified manner not only streamlines the model’s architecture but also enhances its capacity to perform tasks requiring intricate cross-modal reasoning, such as referring segmentation and text-to-image synthesis.

5.5. Ablation Study

To prove that each module of our proposed method is effective, we conducted ablation experiments on complex reasoning segmentation tasks. The ablation of different aspects are as follows:

Modules in neural tuning: The quantitative results are presented in Table 3. We observed that removing sparse vector updating (Equation 2), which renders the tuning layers of the sparse task network independent of each other, leads to a drop in performance. This highlights the significance of interlinking different layers of tuning networks, a factor overlooked by prior tuning methods such as LoRA [41] and (IA)³ [42]. Additionally, performance degrades when the SDR strategy is eliminated, indicating that all neurons are activated for all tasks. Finally, we conducted an ablation study on multitask learning. The results show that removing the multitask learning strategy led to a relative decrease in performance. Notably, the vanilla referring segmentation and image captioning tasks appear to contribute more to complex reasoning than the image generation tasks, which corresponds to the visualized results in Figure 2b.

The selection of tuning modules: In Section 3.2, we integrated task guidance into the LLMs for query and value, following established methods [41]. However, this approach is not the sole option. We conducted corresponding ablation studies, with the quantitative results presented in Table 2. The results indicate that integrating task guidance into keys and values tends to result in poorer performance. While performance improves when task guidance is integrated into all query, key, and value modules, the improvement is only marginal compared to when it is integrated solely into query and value. Therefore, to strike a balance between performance and complexity, we opted to perform tuning only on query and value modules (Equation 5).

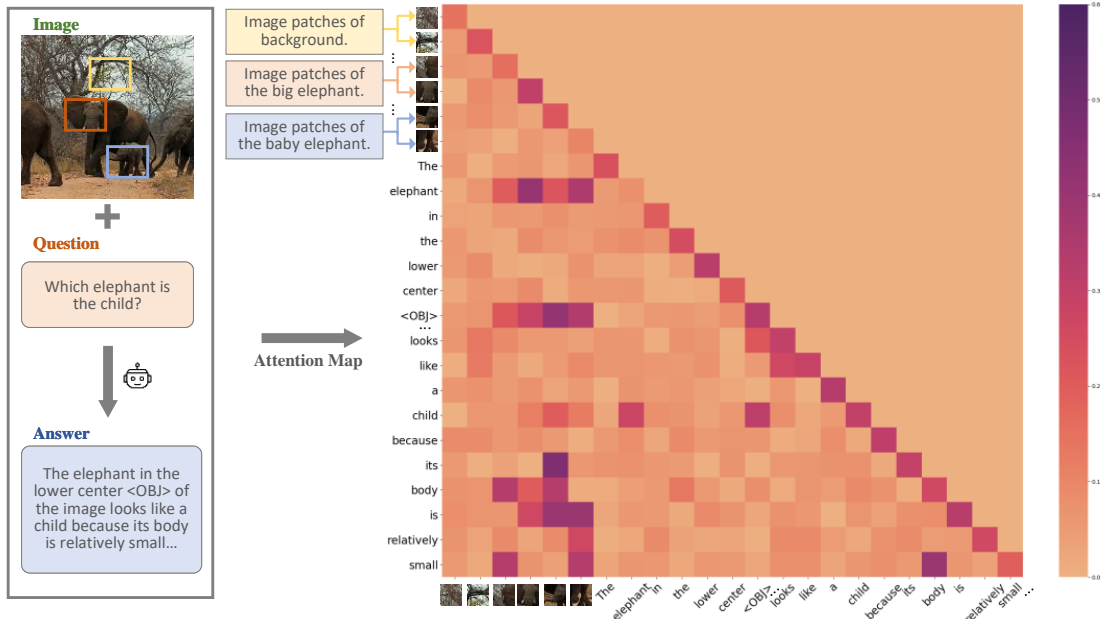


Figure 5: Visualization of Attention Scores for a Reasoning Segmentation Case. For better clarity, we omit the question and answer tokens, as well as some image patches. Darker regions indicate higher attention weights. The results demonstrate that the model effectively builds connections between image details, text, and the ;OBJ_i task token.

Table 4: The ablation of β in sparse vector updating.

Tasks involved	oIoU of Reasoning Segmentation on MMUD									
	$\beta = 0.1$	$\beta = 0.2$	$\beta = 0.3$	$\beta = 0.4$	$\beta = 0.5$	$\beta = 0.6$	$\beta = 0.7$	$\beta = 0.8$	$\beta = 0.9$	$\beta = 1.0$
4 Tasks	62.0	61.9	62.5	62.8	62.1	61.6	60.7	61.0	60.6	61.0
3 Tasks	60.4	60.9	60.7	61.1	62.5	62.5	61.8	61.9	61.2	60.8
2 Tasks	60.0	60.3	60.4	61.2	60.6	61.9	61.7	61.9	62.2	62.0
1 Task	60.1	60.4	59.8	60.7	60.3	60.9	61.5	61.3	61.6	61.7

Choice of image generation decoders: Apart from VQGAN, there are alternative options for image decoding. We also utilized a pre-trained DALL-E2 decoder³ for generating images from the hidden embeddings. A comparison is presented in Figure 4 (Section 5.3). The quality and style of the generated images are significantly influenced by the pre-trained decoders. This bias is a result of the pretraining data used for the decoders. Hence, in theory, neural tuning can employ any pre-trained image synthesis decoder. Unfortunately, due to hardware limitations, we were unable to test other pre-trained models for image generation.

Ablation of β in Sparse Vector Updating The detailed ablations regarding β in sparse vector updating are presented in Table 4. In these experiments, we consistently use the reasoning segmentation task and employ the corresponding oIoU for evaluation. For instance, two tasks involved refer to reasoning segmentation and vanilla segmentation, while only one task involved refers to reasoning segmentation only. From the results, we observe that setting β to 0.4 yields the best performance when all four tasks are involved. For scenarios involving three tasks, the optimal performance is achieved with β set to 0.5 or 0.6. Finally, when there are only one or two tasks, it is more beneficial to activate a higher proportion of neurons, with β set to 0.9 or 1.0.

Ablation of Activation Patterns for Sparse Vector Z_k^u Although we have conducted experiments on the activation rate β of the sparse vector Z_k^u (Appendix 5.5), the activation pattern itself is still worth exploring. In designing

³<http://github.com/hidden/for/review>

Table 5: The ablation of activation patterns for sparse vector. In the experiments, all of four tasks are employed.

Activation Pattern	oIoU of Reasoning Segmentation on MMUD									
	$\beta = 0.1$	$\beta = 0.2$	$\beta = 0.3$	$\beta = 0.4$	$\beta = 0.5$	$\beta = 0.6$	$\beta = 0.7$	$\beta = 0.8$	$\beta = 0.9$	$\beta = 1.0$
Gaussian Random	62.0	61.9	62.5	62.8	62.1	61.6	60.7	61.0	60.6	61.0
Top- 2β Random	61.8	62.0	61.9	62.9	62.7	61.2	61.0	60.9	60.5	59.7
Level Random	61.8	61.7	62.2	62.6	62.6	62.0	60.5	61.0	60.8	59.6
Distribution Random	62.1	60.9	62.5	62.4	60.6	59.8	59.7	60.0	59.6	60.1

our activation strategy, we aimed to activate different neurons according to different tasks and allow the number of activations to fluctuate slightly, mirroring the human thinking process. The simplest and most intuitive approach is to predefine an activation rate and allow it to fluctuate according to a Gaussian distribution, as illustrated in Section 3.2. However, other patterns can also adhere to this activation principle. Below are additional activation strategies explored in our experiments (assuming we need to activate $\beta\%$ of neurons and the fluctuation rate is $f\%$, where $f < \beta$):

- Top- 2β with Random Activation: First, we select the top $2\beta\% \pm 2f\%$ of neurons, then randomly activate $\beta\% \pm f\%$ of neurons within this selected group.
- Level Random Activation: We sort and divide all neurons into 10 levels. In each level, we randomly activate $0.1\beta\% \pm f\%$ of neurons based on task instructions.
- Distribution Random Activation: We define a hyperparameter m , then activate the $\beta\% \pm f\%$ of neurons closest to m (in this approach, we set m to 0 or 1).

The corresponding results for reasoning segmentation are shown in Table 5. Surprisingly, we found that the specific activation strategy had little effect on the results (except the last distribution random activation strategy). Instead, the activation ratio $\beta\%$ had a more significant impact on the final outcomes, indicating that the model can consistently find the neurons it needs. Therefore, to keep the paper concise and easy to understand, we employ the simplest activation strategy in Section 3.2.

6. Conclusion

In this paper, we present a novel unified multimodal multitask learning framework with a new tuning strategy called neural tuning. Under this framework, we unify tasks using an all-in-token approach, which enhances scalability by facilitating the integration of additional modalities or tasks. Additionally, we emulate human cognitive processes through sparse distributed representation, activating specific neurons for different tasks. We evaluate our method across four tasks, including reasoning segmentation and text-to-image synthesis, and demonstrate competitive performance compared to current state-of-the-art methods. To support further research in this area, we introduce the MMUD dataset, which provides a diverse set of annotations for various tasks. Moving forward, we plan to explore additional modalities, such as acoustics, and expand our research into fields like medical applications.

References

- [1] T. Liang, G. Lin, M. Wan, T. Li, G. Ma, F. Lv, Expanding large pre-trained unimodal models with multimodal information injection for image-text multimodal classification, in: Proceedings of the IEEE/CVF conference on computer vision and pattern recognition, 2022, pp. 15492–15501.
- [2] Z. Ren, Z. Huang, Y. Wei, Y. Zhao, D. Fu, J. Feng, X. Jin, Pixellm: Pixel reasoning with large multimodal model, arXiv preprint arXiv:2312.02228 (2023).
- [3] J. Ho, A. Jain, P. Abbeel, Denoising diffusion probabilistic models, in: Advances in Neural Information Processing Systems, Vol. 33, 2020, pp. 6840–6851.
- [4] S. Ahmad, J. Hawkins, How do neurons operate on sparse distributed representations? a mathematical theory of sparsity, neurons and active dendrites, arXiv preprint arXiv:1601.00720 10 (2016).
- [5] A. Spanne, H. Jörntell, Questioning the role of sparse coding in the brain, Trends in neurosciences 38 (7) (2015) 417–427.
- [6] S. Ouyang, H. Wang, S. Xie, Z. Niu, R. Tong, Y.-W. Chen, L. Lin, Slvit: Scale-wise language-guided vision transformer for referring image segmentation, in: Proceedings of the Thirty-Second International Joint Conference on Artificial Intelligence, IJCAI-23, 2023, pp. 1294–1302.

- [7] Z. Huang, X. Wang, L. Huang, C. Huang, Y. Wei, W. Liu, Ccnet: Criss-cross attention for semantic segmentation, in: Proceedings of the IEEE/CVF international conference on computer vision, 2019, pp. 603–612.
- [8] A. Vaswani, Attention is all you need, *Advances in Neural Information Processing Systems* (2017).
- [9] J.-B. Alayrac, J. Donahue, P. Luc, A. Miech, I. Barr, Y. Hasson, K. Lenc, A. Mensch, K. Millican, M. Reynolds, et al., Flamingo: a visual language model for few-shot learning, *Advances in neural information processing systems* 35 (2022) 23716–23736.
- [10] J. Li, D. Li, S. Savarese, S. Hoi, Blip-2: Bootstrapping language-image pre-training with frozen image encoders and large language models, in: International conference on machine learning, PMLR, 2023, pp. 19730–19742.
- [11] J. Y. Koh, R. Salakhutdinov, D. Fried, Grounding language models to images for multimodal inputs and outputs, in: International Conference on Machine Learning, PMLR, 2023, pp. 17283–17300.
- [12] H. Liu, C. Li, Y. Li, Y. J. Lee, Improved baselines with visual instruction tuning, in: NeurIPS 2023 Workshop on Instruction Tuning and Instruction Following, 2023.
- [13] J. Bai, S. Bai, S. Yang, S. Wang, S. Tan, P. Wang, J. Lin, C. Zhou, J. Zhou, Qwen-vl: A frontier large vision-language model with versatile abilities, arXiv preprint arXiv:2308.12966 (2023).
- [14] O. Ronneberger, P. Fischer, T. Brox, U-net: Convolutional networks for biomedical image segmentation, in: Medical image computing and computer-assisted intervention–MICCAI 2015: 18th international conference, Munich, Germany, October 5-9, 2015, proceedings, part III 18, Springer, 2015, pp. 234–241.
- [15] Z. Yang, J. Wang, Y. Tang, K. Chen, H. Zhao, P. H. Torr, Lavt: Language-aware vision transformer for referring image segmentation, in: Proceedings of the IEEE/CVF Conference on Computer Vision and Pattern Recognition, 2022, pp. 18155–18165.
- [16] X. Lai, Z. Tian, Y. Chen, Y. Li, Y. Yuan, S. Liu, J. Jia, Lisa: Reasoning segmentation via large language model, arXiv preprint arXiv:2308.00692 (2023).
- [17] P. Esser, R. Rombach, B. Ommer, Taming transformers for high-resolution image synthesis (2021). arXiv:2012.09841.
- [18] Y. Song, J. Sohl-Dickstein, D. P. Kingma, A. Kumar, S. Ermon, B. Poole, Score-based generative modeling through stochastic differential equations, arXiv preprint arXiv:2011.13456 (2020).
- [19] A. Q. Nichol, P. Dhariwal, Glide: Towards photorealistic image generation and editing with text-guided diffusion models, arXiv preprint arXiv:2112.10741 (2021).
- [20] A. Ramesh, M. Pavlov, G. Goh, S. Gray, C. Voss, A. Radford, M. Chen, I. Sutskever, Zero-shot text-to-image generation, arXiv preprint arXiv:2102.12092 (2021).
- [21] C. Saharia, W. Chan, S. Saxena, L. Li, J. Whang, E. Denton, S. K. S. Ghasemipour, B. K. Ayan, T. Salimans, J. Ho, D. J. Fleet, M. Norouzi, Photorealistic text-to-image diffusion models with deep language understanding, arXiv preprint arXiv:2205.11487 (2022).
- [22] A. Kirillov, E. Mintun, N. Ravi, H. Mao, C. Rolland, L. Gustafson, T. Xiao, S. Whitehead, A. C. Berg, W.-Y. Lo, et al., Segment anything, in: Proceedings of the IEEE/CVF International Conference on Computer Vision, 2023, pp. 4015–4026.
- [23] F. Milletari, N. Navab, S.-A. Ahmadi, V-net: Fully convolutional neural networks for volumetric medical image segmentation, in: 2016 fourth international conference on 3D vision (3DV), Ieee, 2016, pp. 565–571.
- [24] Z. Wang, W. Liu, Q. He, X. Wu, Z. Yi, Clip-gen: Language-free training of a text-to-image generator with clip, arXiv preprint arXiv:2203.00386 (2022).
- [25] T.-Y. Lin, M. Maire, S. Belongie, J. Hays, P. Perona, D. Ramanan, P. Dollár, C. L. Zitnick, Microsoft coco: Common objects in context, in: Computer Vision–ECCV 2014: 13th European Conference, Zurich, Switzerland, September 6-12, 2014, Proceedings, Part V 13, Springer, 2014, pp. 740–755.
- [26] A. Radford, J. W. Kim, C. Hallacy, A. Ramesh, G. Goh, S. Agarwal, G. Sastry, A. Askell, P. Mishkin, J. Clark, et al., Learning transferable visual models from natural language supervision, in: International conference on machine learning, PMLR, 2021, pp. 8748–8763.
- [27] L. Yu, P. Poirson, S. Yang, A. C. Berg, T. L. Berg, Modeling context in referring expressions, in: Computer Vision–ECCV 2016: 14th European Conference, Amsterdam, The Netherlands, October 11-14, 2016, Proceedings, Part II 14, Springer, 2016, pp. 69–85.
- [28] J. Mao, J. Huang, A. Toshev, O. Camburu, A. L. Yuille, K. Murphy, Generation and comprehension of unambiguous object descriptions, in: Proceedings of the IEEE conference on computer vision and pattern recognition, 2016, pp. 11–20.
- [29] V. K. Nagaraja, V. I. Morariu, L. S. Davis, Modeling context between objects for referring expression understanding, in: Computer Vision–ECCV 2016: 14th European Conference, Amsterdam, The Netherlands, October 11–14, 2016, Proceedings, Part IV 14, Springer, 2016, pp. 792–807.
- [30] J. C. Hu, R. Cavicchioli, A. Capotondi, Expansionnet v2: Block static expansion in fast end to end training for image captioning, arXiv preprint arXiv:2208.06551 (2022).
- [31] C. Li, H. Xu, J. Tian, W. Wang, M. Yan, B. Bi, J. Ye, H. Chen, G. Xu, Z. Cao, et al., mplug: Effective and efficient vision-language learning by cross-modal skip-connections, in: Proceedings of the 2022 Conference on Empirical Methods in Natural Language Processing, 2022, pp. 7241–7259.
- [32] K. Papineni, S. Roukos, T. Ward, W.-J. Zhu, Bleu: a method for automatic evaluation of machine translation, in: Proceedings of the 40th annual meeting of the Association for Computational Linguistics, 2002, pp. 311–318.
- [33] R. Vedantam, C. Lawrence Zitnick, D. Parikh, Cider: Consensus-based image description evaluation, in: Proceedings of the IEEE conference on computer vision and pattern recognition, 2015, pp. 4566–4575.
- [34] S. Banerjee, A. Lavie, Meteor: An automatic metric for mt evaluation with improved correlation with human judgments, in: Proceedings of the acl workshop on intrinsic and extrinsic evaluation measures for machine translation and/or summarization, 2005, pp. 65–72.
- [35] M. Heusel, H. Ramsauer, T. Unterthiner, B. Nessler, S. Hochreiter, Gans trained by a two time-scale update rule converge to a local nash equilibrium, *Advances in neural information processing systems* 30 (2017).
- [36] M. Bińkowski, D. J. Sutherland, M. Arbel, A. Gretton, Demystifying mmd gans, in: International Conference on Learning Representations, 2018.
- [37] T. Salimans, I. Goodfellow, W. Zaremba, V. Cheung, A. Radford, X. Chen, Improved techniques for training gans, *Advances in neural information processing systems* 29 (2016).
- [38] J. Yu, Y. Xu, J. Y. Koh, T. Luong, G. Baid, Z. Wang, V. Vasudevan, A. Ku, Y. Yang, B. K. Ayan, et al., Scaling autoregressive models for

- content-rich text-to-image generation, Transactions on Machine Learning Research (2022).
- [39] Y. Li, H. Liu, Q. Wu, F. Mu, J. Yang, J. Gao, C. Li, Y. J. Lee, Gligen: Open-set grounded text-to-image generation, in: Proceedings of the IEEE/CVF Conference on Computer Vision and Pattern Recognition, 2023, pp. 22511–22521.
 - [40] F. Bao, S. Nie, K. Xue, Y. Cao, C. Li, H. Su, J. Zhu, All are worth words: A vit backbone for diffusion models, in: Proceedings of the IEEE/CVF Conference on Computer Vision and Pattern Recognition, 2023, pp. 22669–22679.
 - [41] E. J. Hu, P. Wallis, Z. Allen-Zhu, Y. Li, S. Wang, L. Wang, W. Chen, et al., Lora: Low-rank adaptation of large language models, in: International Conference on Learning Representations, 2021.
 - [42] H. Liu, D. Tam, M. Muqeeth, J. Mohta, T. Huang, M. Bansal, C. A. Raffel, Few-shot parameter-efficient fine-tuning is better and cheaper than in-context learning, Advances in Neural Information Processing Systems 35 (2022) 1950–1965.

Appendix A. Example Appendix Section

Appendix text.